Control by decoherence: weak field control of an excited state objective

2010 New J. Phys. 12 015003

(http://iopscience.iop.org/1367-2630/12/1/015003)

New Journal of Physics
The open-access journal for physics

Control by decoherence: weak field control of an excited state objective

Gil Katz[1], **Mark A Ratner**[2] **and Ronnie Kosloff**[3]

[1] Fritz Haber Research Center for Molecular Dynamics, Hebrew University of Jerusalem, Jerusalem 91904, Israel
[2] Department of Chemistry, Northwestern University, Evanston, IL 60208-3113, USA
[3] Institute of Chemistry and Fritz Haber Research Center for Molecular Dynamics, Hebrew University of Jerusalem, Jerusalem 91904, Israel
E-mail: gkatz@fh.huji.ac.il, ratner@chem.northwestern.edu and ronnie@fh.huji.ac.il

New Journal of Physics **12** (2010) 015003 (13pp)
Received 1 September 2009
Published 19 January 2010
Online at http://www.njp.org/
doi:10.1088/1367-2630/12/1/015003

Abstract. Coherent control employing a broadband excitation is applied to a branching reaction in the excited state. In a weak field for an isolated molecule, a control objective is only frequency dependent. This means that phase control of the pulse cannot improve the objective beyond the best frequency selection. Once the molecule is put into a dissipative environment a new timescale emerges. In this study, we demonstrate that the dissipation allows us to achieve coherent control of branching ratios in the excited state. The model studied contains a nuclear coordinate and three electronic states: the ground and two coupled diabatic excited states. The influence of the environment is modeled by the stochastic surrogate Hamiltonian. The excitation is generated by a Gaussian pulse where the phase control introduced a chirp to the pulse. For sufficient relaxation, we find significant control in the weak field depending on the chirp rate. The observed control is rationalized by a timing argument caused by a focused wavepacket. The initial non-adiabatic crossing is enhanced by the chirp. This is followed by energy relaxation which stabilizes the state by having an energy lower than the crossing point.

Contents

1. Introduction

Coherent control was conceived as a method to actively influence the outcome of a chemical reaction. The basic idea is to generate an interference of matter waves so that a constructive interference is induced in the desired outcome and a destructive interference in all other terminal channels. From this description it is clear that at least two interference pathways constitute the necessary condition for coherent control [1, 2].

Specifically we consider a large molecule with two distinct conformers in the excited electronic state. Such a molecule could be the bacteriorhodopsin, where the final outcomes are the *cis*-/*trans*-branching conformers [3, 4], or two conformers of a dye molecule [5]. Our target of control is then the branching ratio between the two molecular conformers.

What are the control prospects of an isolated molecule? One possibility is to employ a pump–dump scheme, where the first pulse transfers amplitude to the electronic excited state and the second pulse after an appropriate time delay stabilizes the state in the desired conformer [6, 7]. Many variants of this mechanism are possible, which include both shaping the pump and the dump pulses [8, 9]. It is clear from the description that this mechanism requires at least two interactions with the control field to setup the necessary interference [10]. One may ask: is it possible to control the conformer outcome with a single weak shaped pulse? The clear answer is no [11]. It is not possible to exceed the optimal outcome obtained by energetically selecting the best continuous wave (CW) transition determined by the Franck–Condon overlap between the initial state and the final target state.

Is this restriction still relevant when the molecule is immersed in a condensed phase environment? Recently there have been experimental reports of weak field control of large molecules in solution [3]–[5]. The main feature of the control pulse is a negative chirp. The amount of control reported varies from a few per cent to a factor of 1.5 [5]. These findings were criticized on the basis that weak field control is impossible [12, 13]. A clue to explain these results can be found in the recent study of van der Walle *et al* [5]. In this experiment, first the optimal pulse was established for a dye molecule in a specific solvent, then the same pulse was applied to a series of different solvents. As a result, the target of control, i.e. the branching ratio, varied significantly. This finding suggests that the mechanism of control involves the environment [14, 15].

The purpose of this study is to demonstrate that weak field control is feasible in open system dynamics in a system–bath configuration. Only phase control of the pulse is employed. It will be shown that a weak field chirped pulse can significantly control the branching ratio provided the environment can stabilize the outcome on a short timescale. A Hamiltonian description of the bath is employed, which can rule out artefacts that are due to a reduced system–bath description.

2. The model

The model describes a molecular system coupled to a radiation field. It could describe a simplified model of a dye molecule in solution [5]. The molecular system Hamiltonian $\hat{\mathbf{H}}_{\mathrm{S}}$ consists of a ground electronic state and bright and dark excited electronic states:

$$\hat{\mathbf{H}}_{\mathrm{S}} = \begin{pmatrix} \hat{\mathbf{H}}_{\mathrm{g}} & \hat{\boldsymbol{\mu}}_{\mathrm{gb}}\epsilon(t) & 0 \\ \hat{\boldsymbol{\mu}}_{\mathrm{bg}}\epsilon^{*}(t) & \hat{\mathbf{H}}_{\mathrm{b}} & \hat{\mathbf{V}}_{\mathrm{bd}} \\ 0 & \hat{\mathbf{V}}_{\mathrm{db}} & \hat{\mathbf{H}}_{\mathrm{d}} \end{pmatrix}, \tag{1}$$

where $\hat{\mathbf{H}}_k = (\hat{\mathbf{P}}^2/2\mu) + \hat{\mathbf{V}}_k$ is the surface Hamiltonian $k = \{\mathrm{g}, \mathrm{b}, \mathrm{d}\}$, where 'g' is ground, 'b' is bright and 'd' is dark, $(\hat{\mathbf{P}}^2/2\mu)$ is the molecular kinetic energy, where μ is the reduced mass. $\hat{\mathbf{V}}_k(r)$ is the surface potential, where r is the internuclear distance. $\hat{\mathbf{V}}_{\mathrm{bd}}(r)$ represents the non-adiabatic potential coupling the bright and dark electronic surfaces. $\hat{\boldsymbol{\mu}}_{\mathrm{gb}}(r)$ represents the transition dipole operator chosen to couple only the ground and the bright excited state. $\epsilon(t)$ represents the time-dependent electromagnetic field that is the control function in this setup. The target of control is chosen as the asymptotic population ratio between the two bright and dark states.

The molecular system is subject to dissipative forces due to coupling to a primary bath. In turn, the primary bath is subject to interactions with a secondary bath:

$$\hat{\mathbf{H}}_{\mathrm{T}} = \hat{\mathbf{H}}_{\mathrm{S}} + \hat{\mathbf{H}}_{\mathrm{B}} + \hat{\mathbf{H}}_{\mathrm{B}''} + \hat{\mathbf{H}}_{\mathrm{SB}} + \hat{\mathbf{H}}_{\mathrm{BB}''}, \tag{2}$$

where $\hat{\mathbf{H}}_{\mathrm{S}}$ is the system, $\hat{\mathbf{H}}_{\mathrm{B}}$ is the primary bath, $\hat{\mathbf{H}}_{\mathrm{B}''}$ is the secondary bath, $\hat{\mathbf{H}}_{\mathrm{SB}}$ is the system–bath interaction and $\hat{\mathbf{H}}_{\mathrm{BB}''}$ is the primary/secondary bath interaction. Figure 1 presents the system Hamiltonian and the different couplings. The isolated case contains $\hat{\mathbf{H}}_{\mathrm{S}}$ alone. The bath is constructed by employing the stochastic surrogate Hamiltonian [16]. The primary bath Hamiltonian is composed of a collection of two-level systems (TLS).

$$\hat{\mathbf{H}}_{\mathrm{B}} = \sum_j \omega_j \hat{\boldsymbol{\sigma}}_j^{+} \hat{\boldsymbol{\sigma}}_j. \tag{3}$$

The energies ω_j represent the spectrum of the bath. The system–bath interaction $\hat{\mathbf{H}}_{\mathrm{SB}}$ can be chosen to represent different physical processes [17]–[19]. Specifically, we choose an interaction leading to vibrational relaxation:

$$\hat{\mathbf{H}}_{\mathrm{SB}} = \hat{\mathbf{A}}_{\mathrm{S}} \otimes \sum_j^N \lambda_j (\hat{\boldsymbol{\sigma}}_j^{\dagger} + \hat{\boldsymbol{\sigma}}_j), \tag{4}$$

where $\hat{\mathbf{A}}_{\mathrm{S}}$ is the system operator chosen as a function of the amplitude $f(r)$. λ_j is the system–bath coupling parameter of bath mode j. When the system–bath coupling is characterized by a spectral density $J(\omega)$ then $\lambda_j = \sqrt{J(\omega_j)/\rho_j}$ and $\rho_j = (\omega_{j+1} - \omega_j)^{-1}$ is the density of bath modes. We choose an Ohmic bath $J(\omega) = \mu\gamma\omega$ constructed as in [16]. This system bath description for vibrational relaxation has been established by comparing to other

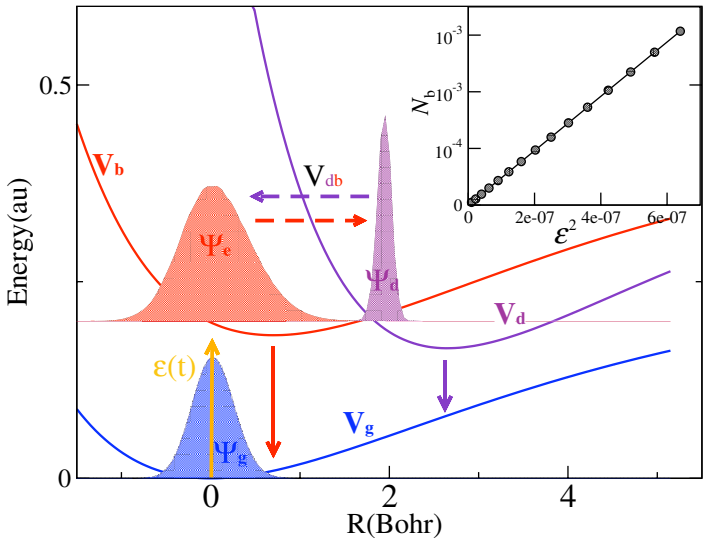

Figure 1. The general scheme: the ground state $\hat{\mathbf{V}}_{\mathrm{g}}(r)$, the bright excited state $\hat{\mathbf{V}}_{\mathrm{b}}(r)$ and the dark excited state $\hat{\mathbf{V}}_{\mathrm{d}}(r)$. Superimposed are snapshots of three wavefunctions: the initial ground state density $\rho_{\mathrm{g}}(r, r)$, the bright state density after the pulse is over $\rho_{\mathrm{b}}(r, r)$ and the dark state density after the transfer $\rho_{\mathrm{d}}(r, r)$ (renormalized). The dotted lines present the absorption and emission from the different final states. The ratio between long time emission of the bright and dark states is an experimental indication of the population ratio between these states. The inset shows the population on the bright state N_{b} as a function of intensity Ω_0^2 indicating that the calculations within this intensity range are performed in the linear regime.

benchmark calculations by Nest *et al* [20], which employed a bath of harmonic oscillators and the multi-configuration time-dependent Hartree (MCTDH) scheme. In turn, they also compared their scheme to a bath description based on a quantum dynamical semigroup [21, 22]. They found that the relaxation dynamics after an initial slippage fits well the Markovian description of the quantum dynamical semigroup. In order to extend the scope of the system–bath dynamics to thermal equilibrium a secondary bath is added.

The secondary bath is also composed of non-interacting TLS at temperature T with the same frequency spectrum as the primary bath. At random times, primary and secondary bath modes of the same frequency are swapped [16]. The swap operator $\hat{\mathbf{S}}$ is defined as

$$\hat{\mathbf{S}}\psi_{\mathrm{B}_j} \otimes \phi_{\mathrm{B}_j''} = \phi_{\mathrm{B}_j} \otimes \psi_{\mathrm{B}_j''}. \tag{5}$$

In a full swap operation, the primary bath mode is reset to a state ϕ with thermal amplitudes and random phases:

$$\phi_j = \frac{1}{\sqrt{2\cosh[\hbar\omega_j/2k_{\mathrm{B}}T]}} \begin{pmatrix} \mathrm{e}^{-(\hbar\omega_j/4k_{\mathrm{B}}T)+\mathrm{i}\theta_1} \\ \mathrm{e}^{+(\hbar\omega_j/4k_{\mathrm{B}}T)+\mathrm{i}\theta_2} \end{pmatrix}, \tag{6}$$

Table 1. Parameters of the calculation. The electronic states are chosen as Morse potentials where: $\hat{\mathbf{V}}_k(r) = D_k(1 - \exp(-\alpha_i(r - \bar{r}_k))^2) + E_k$, where k is the surface index. $\hat{\mathbf{V}}_{\mathrm{bd}}(r) = D_c \cdot \exp(-\alpha_c(r - \bar{r}_c)^2)$. The initial state is the vibrational ground state of $\hat{\mathbf{V}}_{\mathrm{g}}(r)$ obtained by propagation in imaginary time [27]. The system wavefunction is represented on a Fourier grid of N_r points [28]. Propagation is carried out by the Chebychev method [29].

	Typical values	Units
Potential parameters		
D_{g}	3.5	eV
α_{g}	0.3	Bohr^{-1}
$\bar{r}_{\mathrm{g}}$	0	Bohr
E_{g}	0	eV
D_{b}	3.5	eV
α_{b}	0.38	Bohr^{-1}
$\bar{r}_{\mathrm{b}}$	0.	Bohr
E_{b}	4.3	eV
D_{d}	3.5	eV
α_{d}	0.35	Bohr^{-1}
$\bar{r}_{\mathrm{d}}$	2.6	Bohr
E_{d}	4.5	eV
D_{c}	0.1	eV
α_{c}	0.2	Bohr^{-2}
$\bar{r}_{\mathrm{c}}$	1.75	Bohr
Grid parameters		
Grid spacing (Δr)	0.03125	Bohr
Number of grid points (N_r)	128	
Time steps during the pulse (Δt)	0.004	fs
Time steps after the pulse (Δt)	0.5	fs
Order of Chebychev polynomials	128	
Reduced mass (μ)	1836	au
Bath parameters		
Number of bath modes	12	
Cut-off frequency (ω_{c})	1.6	eV
System–bath coupling (γ)	1.945	
Swap rate (Γ/λ)	1.05	

where θ_1, θ_2 are random phases. As a consequence energy is exchanged between the primary and secondary bath at a rate κ_j out of mode j, $\kappa_j = \Gamma_j \hbar\omega_j \frac{1}{2} \coth[\hbar\omega_j/2k_{\mathrm{B}}T]$, where Γ_j is the rate of stochastic swaps. The rate κ_j should be larger than the rate of energy transfer from the primary system to the primary bath $\Gamma_j \geqslant \lambda_j$. Each swap operation resets the phase of the j mode, thus collapsing the system–bath state to an uncorrelated product with the j mode. Accumulating many such random events is equivalent to dephasing [23]. When increasing the number of bath modes to obtain convergence, λ_j and with it Γ_j decrease with the inverse root of the density of bath modes $1/\sqrt{\rho_j}$. The term Γ_j/λ_j determines the ratio between the energy relaxation and the dephasing rate. Table 1 summarizes the parameters of the model and numerical details. At each

instance, the reduced density operator of the system $\hat{\rho}_s$ can be obtained by taking the partial trace over all bath degrees of freedom and averaging over the stochastic realizations:

$$\hat{\rho}_s = \frac{1}{L}\sum_{k}^{L} \mathrm{tr}_B\{|\Psi_{S\otimes B}(k)\rangle\langle\Psi_{S\otimes B}(k)|\}, \tag{7}$$

where L is the number of stochastic realizations and $\Psi_{S\otimes B}(k)$ is the many-body system bath wavefunction of realization k.

An important issue in demonstrating week field control is to eliminate possible artefacts originating from the system–bath reduction scheme. A common approach is to induce a Markovian approximation for the system dynamics. Such an approach is inherent in the Redfield equations [24] or in the adoption of Lindblad equations [21]. The stochastic surrogate Hamiltonian approach overcomes this problem. The system–bath model is based on a non-Markovian Hamiltonian wavefunction construction. Also typically the weak coupling reduction scheme assumes an uncorrelated initial state. In the surrogate Hamiltonian approach, a correlated initial state is generated by propagating in imaginary time [25].

A major possible artefact in most reduction system–bath schemes is that the external control field is not included in the reduction scheme and therefore the system bath relaxation terms are field independent. This issue has been addressed by Meier and Tannor [26]. The surrogate Hamiltonian solves this problem due to the fact that the control pulse is applied to the combined system–bath. Finally convergence of the model is checked by increasing the number of bath modes and the number of stochastic realizations.

3. Control

The target of control is chosen as the asymptotic population ratio of the bright and dark excited states N_d/N_b, where N_b, N_d represent the population on the bright/dark states. Experimentally this ratio is extracted from the accumulated long time spontaneous emission emerging from the bottom of the bright and dark states.

The reference uncontrolled benchmark is initiated by a weak field transform limited Guassian pulse. After such an initial pulse, for the isolated molecular system, the population on the diabatic electronic states are transients since $\hat{\mathbf{N}}_b$ and $\hat{\mathbf{N}}_d$ do not commute with $\hat{\mathbf{V}}_{db}$. These phenomena are illustrated in figure 2 showing major oscillations of the populations N_b and N_d with a frequency ν_{bd}/C of 40 cm^{-1}. This frequency is associated with the magnitude of the non-adiabatic coupling $\hat{\mathbf{V}}_{bd}$. The high frequency minor oscillations correspond to the vibrational frequencies $\nu_{b/d}$ of the bright and dark states, i.e. $\nu_b = 945\,cm^{-1}\,C$ and $\nu_d = 954\,cm^{-1}\,C$.

For an isolated molecular system, the only possible weak field control is to alter the carrier frequency of the pulse. This in turn will populate different vibration eigenstates of the combined coupled excited state potentials. Control will be achieved by choosing an energy which accidentally has a large projection on one or the other diabatic states of a single potential. Modifying the phase of individual spectral components of the pulse will have no effect. In all further calculations, the spectral component and the integrated intensity of the excitation pulse are kept constant.

Coupling the system to a bath introduces a new opportunity for control. Vibrational relaxation leads to stable population at the bottom of each excited potential well thus stopping the oscillations. Figure 2 compares the population oscillations with and without the bath for a

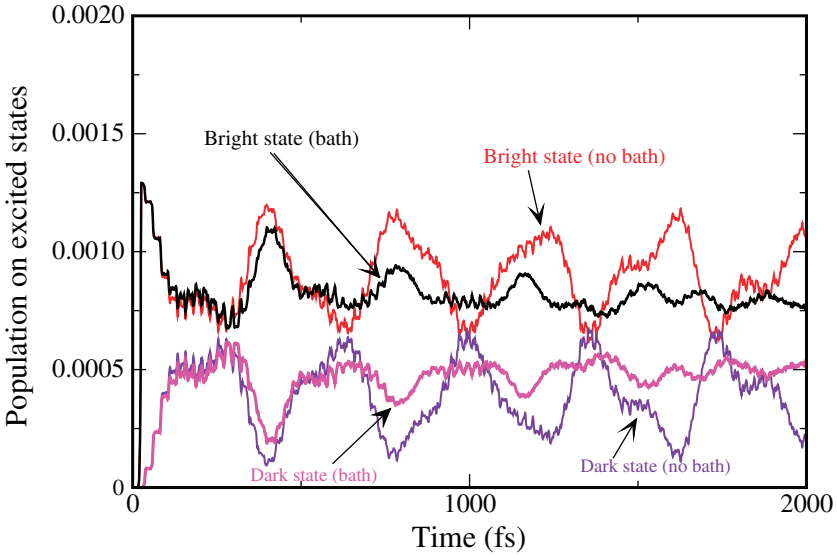

Figure 2. Population as a function of time in the bright N_b (red and black) and dark states N_d (magenta and purple) for a transform-limited pulse. The population in the free system (red and purple) shows a quasi-periodic modulation (typical period of ~ 400 fs). With relaxation the population stabilizes (black and magenta). The bath energy relaxation timescale is $T_1 = 270$ fs.

transform limited pulse. The benchmark free dynamics shows undamped oscillators. The bath leads to a stabilization of the population in each of the diabatic potentials after approximately 2 ps. Figure 3 compares the position and momentum of the projected states on the bright and dark potentials. The stabilization is due to relaxation of momentum to an average value of zero and the position stabilizes at the bottom of each well.

Control is demonstrated by employing a weak Gaussian pulse. The intensity is maintained within the linear regime (cf figure 1). The total excitation of population is limited to the range of $N_b \sim 10^{-3}$. Only the spectral phase is controlled, meaning the amplitude of the spectral components of the pulse are preserved. For simplicity, we choose a pulse for which the control knob is the chirp. For this pulse, the time-dependent electric field $\epsilon(t)$ becomes [30]:

$$\epsilon(t) = \tilde{\Omega}_0 \exp\left[-\frac{t^2}{\tau_0^2 + 2i\phi''} + i\omega_0 t\right] = \frac{\Omega_0}{w_F} \exp\left[-\frac{t^2}{w_F^2 \tau_0^2} + i\frac{1}{2}\chi t^2 + i\omega_0 t\right], \qquad (8)$$

where ω_0 is the carrier frequency, τ_0 is the transform limit (TL) temporal width of the pulse, ϕ'' is its group velocity dispersion (GVD), τ is the actual temporal width, such that $\tau = \tau_0 w_F$, where w_F is the broadening factor. χ is the chirp rate and Ω_0 is the TL peak field. The parameters of the calculation are $\hbar\omega_0 = 5.2$ eV, $\tau_0 = 12$ fs, $\chi_{max} = 0.0184\,\text{fs}^{-2}$, $\Omega_0 = 0.005$ au and a broadening factor $w_f = 1.38$. The numerical parameters of the propagation and bath are summarized in table 1. The same bath parameters are used for the three surfaces.

Figure 4 displays the branching ratio N_d/N_b as a function of chirp parameter χ. When the bath is absent as expected the chirp has no influence on the branching ratio. The small oscillations reflect the continuing oscillations of population from the bright to the dark states (cf figure 2). As a result it is difficult to determine the exact average population. Once relaxation is

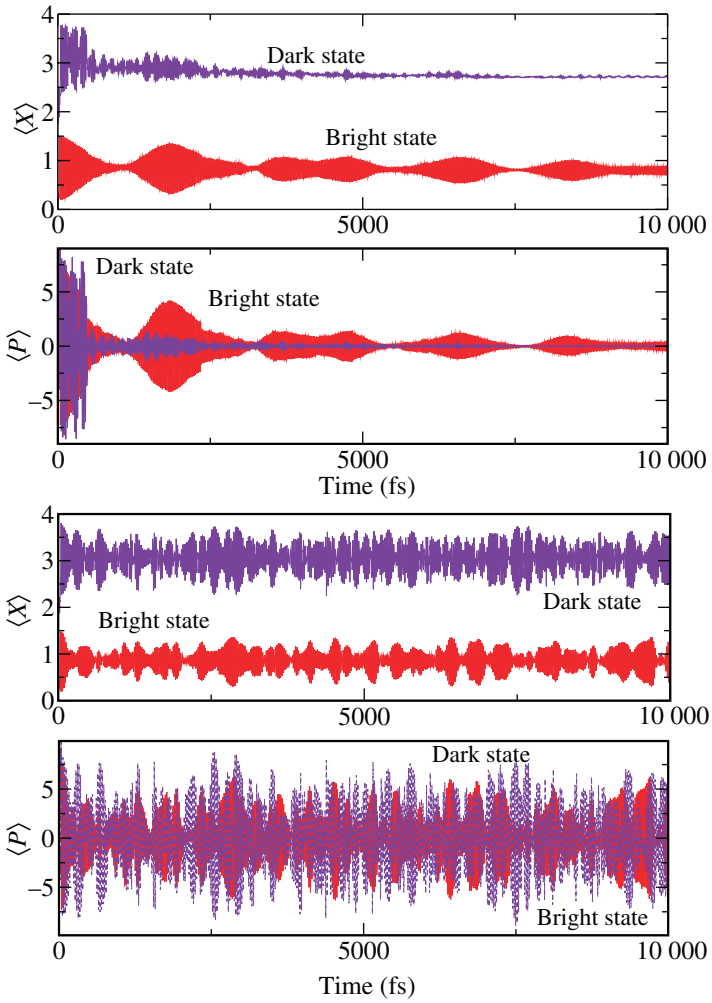

Figure 3. Position and momentum expectation values as a function of time for the bright state (red) and the dark state (purple) with (upper panel) and a free system without a bath (lower panel). The result for a transform limited pulse is shown. The T_1 of the bath is 270 fs.

set, the population on each excited state stabilizes. Convergence of the calculations with respect to the bath were checked by increasing the number of bath modes and the number of realizations. In addition, the calculations were compared to a non-stochastic surrogate Hamiltonian with 48 bath modes. Convergence of the branching ratio N_d/N_b at 5 ps was within 1.4% for 9 bath modes and 10 realizations and 0.9% for 12 bath modes and 10 realizations.

Examining figure 4, we observe that when there is sufficient system–bath coupling, only phase control is possible. Positive chirp suppresses the dark state while negative chirp enhances with respect to the TL pulse (no chirp), which is similar to free propagation ratio $N_d/N_b \sim 0.35$. The maximum effect is obtained when the timescale of energy relaxation matches the oscillation period bright/dark population transfer. When the system–bath coupling further increases, a turnover is observed and the ratio N_d/N_b decreases (see the inset of figure 4). In addition, the control is lost. In this case, the strong dissipation destroys the coherence and stabilizes the product in the first bright well. The turnover is reminiscent of phenomena observed in electron

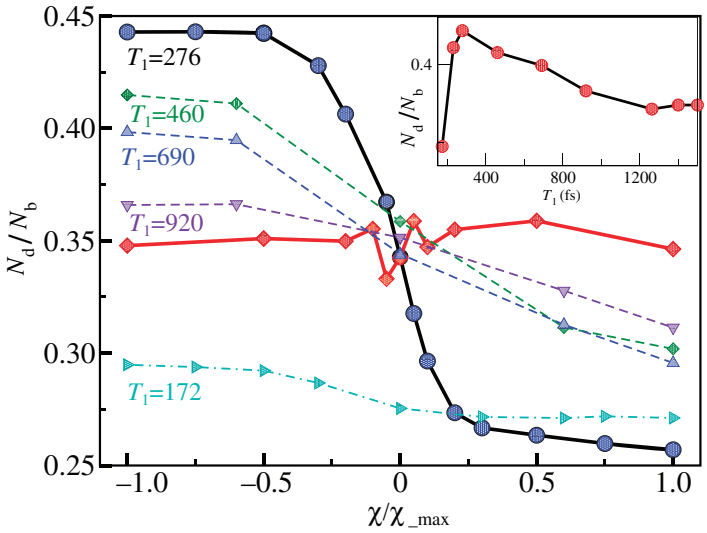

Figure 4. Branching ratio between the bright and dark state as a function of the chirp rate $\chi/\chi_{\max}$, ($\chi_{\max} = 0.0184\,\mathrm{fs}^{-2}$). The branching ratio is defined as the ratio of population N_d/N_b on each state at 7 ps. Each line corresponds to a different system–bath coupling value characterized by T_1 in fs the energy relaxation timescale. The solid red line corresponds to the reference free system. The inset shows the branching ratio between dark and bright states for $\chi/\chi_{\max} = -1.0$ for different system–bath coupling energy relaxation times T_1 in fs.

transfer [18, 31, 32]. One should mention that in weak field conditions, the total population transfer from the ground to the excited states is independent of chirp. When the intensity is increased, negative chirp leads to minimum population transfer [33]–[38]. The present phase control is not optimal. We expect that employing optimal control theory (OCT) either in a weak field or in more intense conditions will lead to significant enhancement of the control as was found for curve crossing systems [39].

The question remaining is: what is the influence of the chirp? The main effect of a chirped pulse on the excited state is to focus the wavefunction on the crossing point (see figure 5 [40]). The relaxation then plays the role of a dump pulse that stabilizes the product by dissipating energy below the crossing point. Figure 6 compares the population transfer rate $\mathrm{d}N_d/\mathrm{d}t$ as a function of time for positive, negative and zero chirp half a vibrational period after the excitation pulse. Although the transfer rate $\mathrm{d}N_d/\mathrm{d}t = (2/\hbar)\langle\psi_d|\hat{\mathbf{V}}_{db}|\psi_b\rangle$ [41] oscillates considerably, the amplitude of the negative chirp case is significantly larger. The accumulated population on the dark state reflects this trend.

The mechanism of control can be understood as follows: the population transfer in the first few vibrational periods is most effective. The transferred wavefunction is reflected from the outer turning point of the dark state and collides again with the crossing region. During this period dissipation takes place. As a result the system energy approaching the crossing point is reduced. For conditions where the initial energy is slightly below the crossing point, the non-adiabatic crossing is in the tunneling regime [42]. A decrease in energy will exponentially reduce the back transfer to the bright state. Further relaxation will stabilize the product. Amplitude that was reflected from the crossing in the first pass will lose energy in the bright state

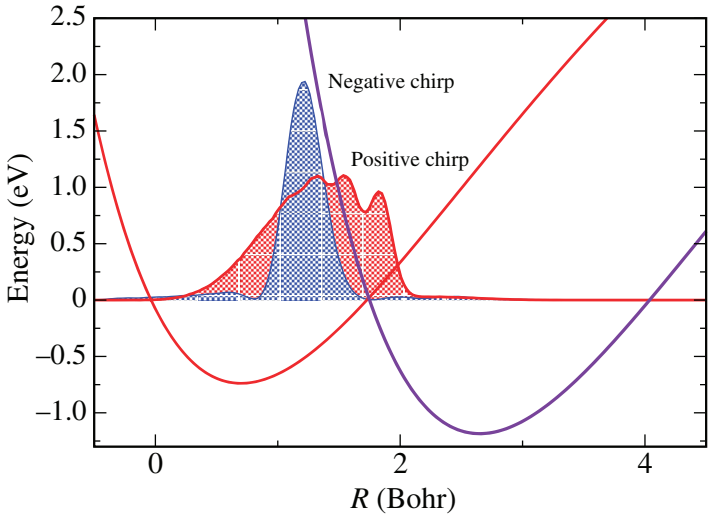

Figure 5. The focused and defocused wavepackets on the bright state superimposed on the potentials. The negative chirp is in blue and the positive chirp in red corresponding to $\pm\chi_{\max}$. The time corresponds to half a vibrational period after the pulse.

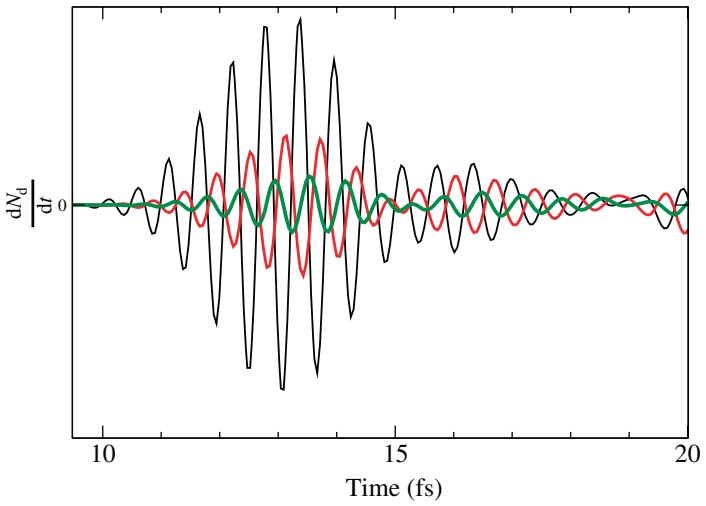

Figure 6. The population transfer rate $\langle \mathrm{d}N_\mathrm{d}/\mathrm{d}t\rangle = -\langle \mathrm{d}N_\mathrm{b}/\mathrm{d}t\rangle = (2/\hbar)\mathrm{Im}\{\langle\psi_\mathrm{d}|\hat{\mathbf{V}}_\mathrm{db}|\psi_\mathrm{b}\rangle\}$ as a function of time after the excitation pulse for negative (blue), positive (red) and no chirp (black). Note the phase shift between the different chirps. The maximum amplitude occurs approximately half a vibrational period after the pulse.

reducing its crossing probability on the second pass. The mechanism can now be understood as a timing control. The negative chirp enhances the population transfer in the first non-adiabatic transfer event. Due to energy loss to the bath subsequent passes have a lower crossing probability.

4. Conclusions

Weak field control has been an outstanding issue in recent years. Experimental demonstrations require a sufficient theory. To this end, we constructed a minimum molecular model constructed from ground, bright and dark electronic states. As a freely propagating system, we confirm that there is no phase control in a weak field. Coupling to the bath changes the control perspective. To eliminate artefacts, we choose a non-Markovian system bath description cast into a stochastic wavefunction formalism. Convergence is obtained by increasing the number of bath modes. The bath introduces a new timescale of energy relaxation. When this timescale becomes comparable to the timescale of non-adiabatic population transfer an opportunity for coherent control emerges. We demonstrated a simple mechanism where a negative-chirped pulse focuses the wavefunction on the crossing point enhancing the first passage transfer. Dissipation acts like a dump pulse and stabilizes the products in an early stage. When the dissipative becomes too strong the wavefunction cannot survive the first crossing without losing energy, leading to a product stabilized in the bright state and loss of control.

Acknowledgments

We thank Valentyn Prokhorenko and Misha Ivanov for helpful discussion. We are grateful to the Niedersachsen/Israel grant and the DOE/EFRC program, for support of this work.

References

[1] Gordon R and Rice S 1997 Active control of the dynamics of atoms and molecules *Annu. Rev. Phys. Chem.* **48** 601

[2] Brumer P W and Shapiro M 2003 *Principles of the Quantum Control of Molecular Processes* (New York: Wiley)

[3] Prokhorenko V, Nagy A M and Dwayne Miller R J 2005 Coherent control of the population transfer in complex solvated molecules at weak excitation: an experimental study *J. Chem. Phys.* **122** 184502

[4] Prokhorenko V, Nagy A M, Waschuk S A, Brown L S, Birge R R and Dwayne Miller R J 2006 Coherent control of retinal isomerization in bacteriorhodopsin *Science* **313** 1257

[5] van der Walle P, Milder M T W, Kuipers L and Herek J L 2009 Quantum control experiment reveals solvation-induced decoherence *Proc. Natl Acad. Sci. USA* **106** 7714

[6] Tannor D J and Rice S A 1985 Control of selectivity of chemical-reaction via control of wave packet evolution *J. Chem. Phys.* **83** 5013

[7] Tannor D J, Kosloff R and Rice S 1986 Mode selective chemistry by a two photon process *J. Chem. Phys.* **85** 5805–20

[8] Kosloff R, Rice S A, Gaspard P, Tersigni S and Tannor D 1989 Wavepacket dancing: achieving chemical selectivity by shaping light pulses *Chem. Phys.* **139** 201–20

[9] Rabitz H, de Vivie-Riedle R, Motzkus M and Kompa K 2000 Chemistry—whither the future of controlling quantum phenomena? *Science* **288** 824

[10] Yan Y J, Gillilan R E, Whitnell R M, Wilson K R and Mukamel S 1993 Optical control of molecular dynamics: Liouville-space theory *J. Phys. Chem.* **97** 2320

[11] Brumer P and Shapiro M 1989 One photon mode selective control of reactions by rapid or shaped laser-pulses—an emperor without clothes *Chem. Phys.* **139** 221

[12] Joffre M 2007 Comment on: Coherent control of retinal isomerization in bacteriorhodopsin *Science* **317** 453
[13] Prokhorenko V, Nagy A M, Waschuk S A, Brown L S, Birge R R and Dwayne Miller R J 2006 Response to comment: Coherent control of retinal isomerization in bacteriorhodopsin *Science* **317** 453
[14] Wu L-A, Bharioke A and Brumer P 2008 Quantum conditions on dynamics and control in open systems *J. Chem. Phys.* **129** 041105
[15] Hoki K and Brumer P 2009 Dissipation effects on laser control of *cis/trans* somerization *Chem. Phys. Lett.* **468** 23
[16] Katz G, Gelman D, Ratner M A and Kosloff R 2008 Stochastic surrogate Hamiltonian *J. Chem. Phys.* **129** 034108
[17] Baer R, Zeiri Y and Kosloff R 1997 Hydrogen transport in nickel (111) *Phys. Rev.* B **55** 10952
[18] Koch C P, Kluner T and Kosloff R 2002 A complete quantum description of an ultrafast pump–probe charge transfer event in condensed phase *J. Chem. Phys.* **116** 7983–96
[19] Koch C P, Klüner T, Freund H-J and Kosloff R 2003 Femtosecond photodesorption of small molecules from surfaces: a theoretical investigation from first principles *Phys. Rev. Lett.* **90** 117601
[20] Nest M and Meyer H-D 2003 Dissipative quantum dynamics of anharmonic oscillators with the multiconfiguration time-dependent Hartree method *J. Chem. Phys.* **119** 24
[21] Lindblad G 1976 Generators of quantum dyanamical semigroups *Commun. Math. Phys.* **48** 119
[22] Gorini V, Kossokowski A and Sudarshan E C G 1976 Completely positive dynamical semigroups of n-level systems *J. Math. Phys.* **17** 821
[23] Khasin M and Kosloff R 2008 The globally stable solution of a stochastic nonlinear Schrödinger equation *J. Phys. A: Math. Gen.* **41** 365203
[24] Redfield A G 1957 On the theory of relaxation processes *IBM J.* **1** 19
[25] Gelman D and Kosloff R 2003 Simulating dissipative phenomena with a random phase thermal wavefunctions, high temperature application of the surrogate Hamiltonian approach *Chem. Phys. Lett.* **129** 381
[26] Meier C and Tannor D J 1997 Non-Markovian evolution of the density operator in the presence of strong laser fields *J. Chem. Phys.* **111** 3365
[27] Kosloff R and Tal-Ezer H 1986 Direct a relaxation method for calculating eigenfunctions and eigenvalues of the Schrödinger equation on a grid *Chem. Phys. Lett.* **127** 223–30
[28] Kosloff R 1988 Time dependent methods in molecular dynamics *J. Phys. Chem.* **92** 2087–100
[29] Ezer H T and Kosloff R 1984 An accurate and efficient scheme for propagating the time dependent Schrödinger equation *J. Chem. Phys.* **81** 3967–70
[30] Luc-Koenig E, Kosloff R, Masnou-Seeuws F and Vatasescu M 2004 Photoassociation of cold atoms with chirped laser pulses: time-dependent calculations and analysis of the adiabatic transfer within a two-state model *Phys. Rev.* A **70** 033414
[31] Ashkenazi G, Kosloff R and Ratner M A 1999 Photoexcited electron transfer: short-time dynamics and turnover control by dephasing, relaxation and mixing *J. Am. Chem. Soc.* **121** 3386–95
[32] Kosloff R and Ratner M A 2002 Rate constant turnovers: energy spacings and mixings *J. Phys. Chem.* B **106** 8479–83
[33] Cerullo G, Bardeen C J, Wang Q and Shank C V 1996 High-power femtosecond chirped pulse excitation of molecules in solution *Chem. Phys. Lett.* **262** 362–8
[34] Bardeen C J, Wang Q and Shank C V 1998 Femtosecond chirped pulse excitation of vibrational wave packets in ld690 and bacteriorhodopsin *J. Phys. Chem.* A **102** 2759–66
[35] Nahmias O, Bismuth O, Shoshana O and Ruhman S 2005 Tracking excited state dynamics with coherent control: automated limiting of population transfer in lds750 *J. Phys. Chem.* A **109** 8246
[36] Malinovsky V and Krause J L 2001 Efficiency and robustness of coherent population transfer with intense, chirped laser pulses *Phys. Rev.* A **63** 043415

[37] Fainberg B D and Gorbunov V A 2004 Coherent population transfer in molecules coupled with a dissipative environment by intense ultrashort chirped pulse. a simple model *J. Chem. Phys.* **121** 8748
[38] Gelman D and Kosloff R 2005 Minimizing broadband excitation under dissipative conditions: theory and experiment *J. Chem. Phys.* **123** 234506
[39] Gross P, Neuhauser D and Rabitz H 1992 Optimal control of curve-crossing systems *J. Chem. Phys.* **96** 2834
[40] Krause J L, Whitnell R M, Wilson K R, Yan Y and Mukamel S 1993 Optical control of molecular dynamics, molecular cannons, reflectrons and wave-packet focusers *J. Chem. Phys.* **99** 6562
[41] Hammerich A, Kosloff R and Ratner M 1992 Chemistry in strong laser fields. An example from methyl iodide photodissociation *J. Chem. Phys.* **97** 6410
[42] Zhu C Y and Nakamura H 1994 Theory of nonadiabatic transition for general 2-state curve crossing problems 1. Nonadiabatic tunneling case *J. Chem. Phys.* **101** 10630